Available online at www.sciencedirect.com
ScienceDirect
International Journal of Impact Engineering 34 (2007) 1272–1285
INTERNATIONAL JOURNAL OF IMPACT ENGINEERING
www.elsevier.com/locate/ijimpeng

A general elastic–plastic approach to impact analisys for stress state limit evaluation in ball screw bearings return system

Claudio Braccesi, Luca Landi*

Dipartimento di Ingegneria Industriale, Università di Perugia, Via G. Duranti 1/A-4–06125 Perugia, Italy

Received 19 April 2005; received in revised form 12 June 2006; accepted 16 June 2006
Available online 22 August 2006

Abstract

A methodology for stress state limit recovering in ball screws return system is presented in this paper. A lot of different researches and standards have been already performed for rolling bearings load static and dynamic rating (ISO 76, ISO 281), but nothing has been said for ball screws except in some drafting standards (Draft standard DIN 69051-4). Also the overall stress limits introduced for rolling bearings in ISO standards are not valid for ball screws bearing because of their different contact geometry. Moreover, the plastic contact due to impact between the spheres and the ball return system, very important for ball screw bearing life determination, has been investigated in very recent works only for nominal impacts by Hung et al. [Impact failure analysis of re-circulating mechanism in ball screw. Eng Failure Anal 2004;11:561–73].

A general model for the elastic–plastic contact between two curved bodies, derived from the models introduced by Thornton [Coefficient of restitution for collinear collisions of elastic perfectly plastic spheres. ASME J Appl Mech 1997;64:383], and Thornton and Zemin Ning [A theoretical model for the stick/bounce behaviour of adhesive, elastic–plastic spheres. Powder Technol 1998;99:154–62], is introduced in this paper to describe the elastic–plastic impact behaviour of two general curved bodies.

By using this approach the influence on the stress state due to geometric properties, materials and impact velocities is established using an experimental plastic deformation limit. So one can finally estimate an equivalent elastic Hertz stress limit (EHSL) useful for ball screw bearing design through the typical elastic Hertz formulas. Finally the optimal correlation between the EHSL and the experimental results for "conventional" ball bearings is recovered, moreover the EHSL for a lot of different ball screw return systems are evaluated.

Keywords: Elastic–plastic impact; Ball screw stress limit; Contact mechanics

1. Introduction

Equivalent elastic Hertz stresses are a common approach for static load rating determination for ball bearings in all the bearing industries. Using this simple theory one can determine the limit equivalent static stress for a rolling bearing [1] through the Hertz formulas [2] for elastic contact stress between two curved bodies. As it is known the equivalent Hertz stress (EHS) has to be evaluated on the centre of the contact

*Corresponding author. Tel.: +39 075 5853726; fax: +39 075 5853703.
E-mail address: l.landi@unipg.it (L. Landi).

0734-743X/$ - see front matter © 2006 Elsevier Ltd. All rights reserved.
doi:10.1016/j.ijimpeng.2006.06.005

surface between the more loaded rolling body and the rolling raceways, this stress is usually called *maximum Hertz pressure on the contact surface* (p_{max}).

In ball screw design there are two different critical contact zones: the contact zone between the ball nut and the rolling spheres during the "regular" motion and the impact zone at the very beginning of the ball-nut return system where the spheres trajectory is strongly deviated from the nominal one in a little space.

The beginning contact zone has been already studied by ball screw industries both for static and dynamic loads (see for example [3]) and although some draft standard have been also developed [4], nothing is said for the second one.

Experimentations on commercial return systems failure shows a "static failure" (after a few hours of life) due to incremental plastic deformation during the successive spheres impacts that have a considerable effect on the return system nominal geometry. This nominal geometry change causes a rapid increase of the maximum pressure on the contact surface and a considerable decrease of ball screw life.

This early failure is often caused by elastic deformation of the nut-ball (caused by the great loads acting on the screw ball bearing) that modifies the designed nominal contact geometry in the impact zone at the very beginning of the ball-nut return system.

In fact, essentially when the internal return system is cut into the nut (see Fig. 1), the local stiffness of the nut is drastically reduced and some geometry deformation may occur, especially for aeronautical application where considerable vibration (dynamical stresses) have to be taken in account.

The "nominal" fatigue behaviour failure mechanism studied for example in [5] is not sufficient for the design and testing of such screw balls and another approach has to be taken into account also to consider the real contact geometry.

In commercial roller bearing design the equivalent elastic Hertz stress limit (EHSL) for a typical steel material–impact geometry is derived in terms of maximum EHS usually called p_{max}, whose typical limit value is EHSL $\leqslant$ 4200 Mpa, for a nominal elastic impact [6]. Moreover the precise correlation between different materials, real contact angle, impact velocity and geometry of the return system on the early failure mechanism is not known [7].

On recent times some theoretical and numerical models for the stick-bounce behaviour of elastic–plastic spheres were introduced mainly to describe the dependence of the coefficient of restitution in elastic–perfectly plastic impacts of particles [8–12]. The so called normal force displacement (NFD) models proposes different relations for taking into account both the elastic and plastic radii on the contact zone all in one elastic–plastic total radius. In these models two different relations between the elastic–plastic load/unload and an equivalent Hertz one are proposed in terms of load—deformation characteristics (spheres approach).

Moreover the state of the art for static load limit has already been studied through experimental tests, for typical steel materials, in terms of *residual permanent deformation*: $\alpha_p = 0.0001$ of the rolling element diameter (d_w) at the centre of the most heavily stressed element-raceway.

So the main objective of this work is to obtain a general elastic–plastic model for contact between curved bodies from the Thornton NFD one and, through the α_p, to find the EHSL either for roller bearing screw

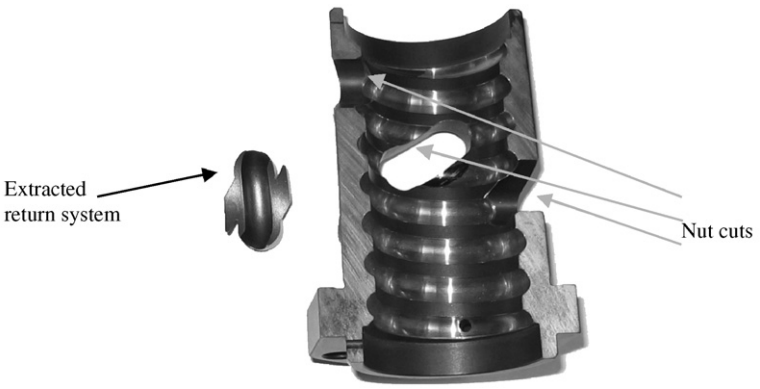

Fig. 1. Typical geometry of a nut with an internal return system.

bearing (to validate the model) and than for a general ball screw return system. The relation between the EHLS and the typical design parameter like materials yield stresses, geometric properties in the contact zone, impact angle, ball screw turning speed will be described also through numerical examples and figures.

2. Elastic–perfectly plastic general model

2.1. Elastic–perfectly plastic spheres contact

The Hertz contact mechanism [2] gives an accurate non-linear model for the elastic contact problem of two different bodies. Calling P the contact force between two spheres of radius R_i, elastic modulus E_i, v_i Poisson coefficient, the Hertz pressure distribution over the circular contact area of radius a is semi-elliptical:

$$p(r) = \frac{3P}{2\pi a^2}\left[1 - \left(\frac{r}{a}\right)^2\right]^{1/2}. \tag{1}$$

The maximum value of the contact pressure is

$$p_{\max} = \frac{3P}{2\pi a^2}. \tag{2}$$

Defining the equivalent elastic modulus and curvature respectively as

$$\frac{1}{E^*} = \frac{1-v_1^2}{E_1} + \frac{1-v_2^2}{E_2} \quad \text{(equivalent elastic modulus)}, \tag{3}$$

$$\frac{1}{R^*} = \frac{1}{R_1} + \frac{1}{R_2} \quad \text{(equivalent curvature)}, \tag{4}$$

the relation between contact force P and relative approach α is given by

$$P = \frac{4}{3}E^* R^{*1/2}\alpha^{3/2}, \tag{5}$$

where

$$a^2 = R^*\alpha. \tag{6}$$

It is also possible to define a *yield contact pressure* $p_{\max} = p_y$ when $a = a_y$, substituting (5) and (6) into (2):

$$p_y = \frac{2E^* a_y}{\pi R^*}. \tag{7}$$

In order to model the perfect plastic behaviour Thornton [8] makes some simplifying assumptions.

Thornton assumption 1. During the plastic deformation the contact pressure distribution is limited by p_y defined in (7). After the material yield it is possible to define an equivalent elastic force P_e as the Hertz contact force which would turn out if all the elastic–plastic contact area πa^2 were in an elastic state. The radius a_p defines the radius of the contact area over which an uniform pressure p_y is assumed, see Fig. 2. The ruling equation for the P_e force is obviously (5).

After the yield, the normal force P is given by

$$P = P_e - 2\pi\int_0^{a_p}\left[p(r) - p_y\right] r\,\mathrm{d}r. \tag{8}$$

Integrating Eq. (8) and considering the condition at yield, Thornton [8] in Eq. (14) finds the relation between the a, a_y and a_p radii and the force–displacement linear relation during plastic loading:

$$a^2 = a_y^2 + a_p^2, \tag{9}$$

$$P = P_y + \pi p_y R^*(\alpha - \alpha_y). \tag{10}$$

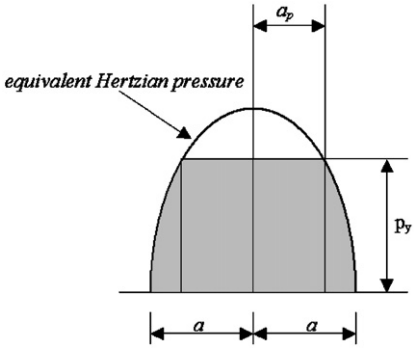

Fig. 2. Thornton pressure distribution for elastic–perfectly plastic spheres.

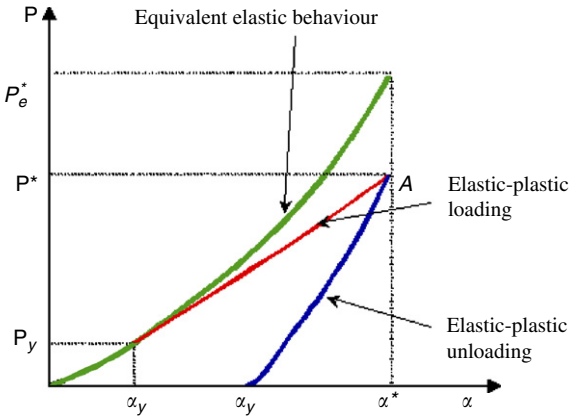

Fig. 3. Thornton force–relative approach relationship for elastic–perfectly plastic spheres.

Eq. (9) states that the elastic–plastic equivalent contact area can be seen as the sum of the yielding limit area and the area given by the plastic contact radius. The very important Eq. (10) states that the plastic component of the elastic–plastic loading curve is a straight line tangent to the elastic one in its starting point (P_y, α_y), see Fig. 3.

During the unloading phase, when a plastic deformation is already occurred, the equivalent plastic radius R_p^* will be greater then the elastic one R^* due to permanent plastic deformation of the contact surfaces. The ruling equation of unloading phase is still (5) but the R_p^* radius has to be used:

$$P = \frac{4}{3} E^* R_p^{*1/2} (\alpha - \alpha_p)^{3/2}, \tag{11}$$

where R_p^* is defined as the equivalent plastic radius in the point of maximum relative approach α^* reached during the compression. This unknown R_p^* radius will be evaluated through one further assumption.

Thornton assumption 2. At unloading point (P^*, α^*), the contact area developed by the actual maximum normal force P^* and reduced curvature $1/R_p^*$ is the same as that which would be generated by an equivalent elastic force P_e^* (elastic equivalent contact force at unloading point) and contact curvature $1/R^*$. Combining Eqs. (5) and (6), we can therefore state:

$$a^3 = \frac{3R^*P}{4E^*}. \tag{12}$$

Using Eq. (11) assumption, area equivalence, can also be written as

$$R_p^* P^* = R^* P_e^*. \tag{13}$$

Summarising, as one can see in Fig. 3, the elastic–plastic loading is tangent in the point (P_y, α_y) to the equivalent elastic one and the unloading reaches the load $P = 0$ with a residual permanent plastic deformation α_p.

Substituting using the Eqs. (5) and (11) for $\alpha = \alpha^*$ into Eq. (13) one can find:

$$R^*\alpha^* = R^*_p(\alpha^* - \alpha_p) \tag{14}$$

and obviously:

$$R^*_p = \frac{\alpha^*}{(\alpha^* - \alpha_p)} R^*. \tag{15}$$

Imposing the experimental permanent deformation: $\alpha_p = 0.0001 d_w$ as a residual deformation limit it is possible to substitute Eq. (15) into (11) and the resulting intersection point A (P^*, α^*) in Fig. 3 can be recursively obtained from the system:

$$\begin{aligned} P^* &= P_y + \pi p_y R^*(\alpha^* - \alpha_y), \\ P^* &= \frac{4}{3} E^* \frac{\alpha^*}{(\alpha^* - \alpha_p)} R^{*1/2}(\alpha^* - \alpha_p)^{3/2}. \end{aligned} \tag{16}$$

Finally the equivalent EHLS (P^*_e) can be obtained from (13).

2.2. Elastic–perfectly plastic bodies contact

The contact between two general curved bodies with four different curvature radii, (ρ_{11}, ρ_{12}) for body 1 and (ρ_{21}, ρ_{22}) for body 2, have to be considered. As it is known the Hertzian elastic theory states that the contact zone is elliptical (with a and b semi axes). The contact pressure distribution is semi-ellipsoidal (see Fig. 4) and it can be written as

$$p(x, y) = p_{max} \sqrt{\left(1 - \left(\frac{x}{a}\right)^2 - \left(\frac{y}{b}\right)^2\right)}, \tag{17}$$

where p_{max} is, as usual, the maximum contact pressure at the ellipse centre (the same of Eq. (2) substituting the ellipse area πab to the circle one πa^2).

It is possible to define the *curvature sum* $(\sum\rho)$ and the *curvature* function $(F(\rho))$ as [6]:

$$\sum \rho = \rho_{11} + \rho_{12} + \rho_{21} + \rho_{22} = 1/R^H, \tag{18}$$

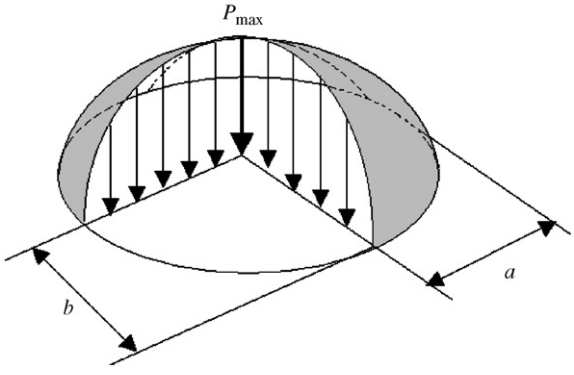

Fig. 4. Contact force distribution for general curved bodies.

$$F(\rho) = \frac{\left|(\rho_{11} - \rho_{12}) + (\rho_{21} - \rho_{22})\right|}{\sum \rho}$$

(for coincident principal plane of the two bodies), (19)

and the *eccentricity* of the ellipse of contact as

$$e = \sqrt{\left(1 - \left(\frac{b}{a}\right)^2\right)}. \tag{20}$$

The force-relative approach relation becomes [6, Eq. (3.20), p. 56]:

$$P = \frac{2\pi}{3k}\sqrt[2]{\frac{2L(e)}{K^3(e)}}E^*\left(R^{\mathrm{H}}\right)^{1/2}\alpha^{3/2} = AE^*\left(R^{\mathrm{H}}\right)^{1/2}\alpha^{3/2}, \tag{21}$$

where K(e) and L(e) are elliptic integral defined on [6, Eqs. (3.8) and (3.11), p. 54]

$$k = b/a \text{ and } A = \frac{2\pi}{3k}\sqrt[2]{\frac{2L(e)}{K^3(e)}}$$

is a number that depends only from the two bodies curvatures ρ_{11}, ρ_{12} and ρ_{21}, ρ_{22}.

In the generalized contact the Thornton *assumptions* are still valid without limitation, with the difference of considering elliptic limit elastic areas instead of circular ones.

Eq. (6) becomes:

$$ab = \left(\frac{2L(e)}{K(e)k}\right)R^{\mathrm{H}}\alpha. \tag{22}$$

So, if the curvature sum of Eq. (18) is known, it is possible to determine the plastic part of the elastic–plastic diagram as the straight line tangent to the elastic one in the $(P_{\mathrm{y}}, \alpha_{\mathrm{y}})$ point whose angular coefficient is, from Eqs. (21) and (22):

$$\left(\frac{\partial P_{\mathrm{el}}}{\partial \delta}\right)_{\delta=\delta_{\mathrm{y}}} = \frac{3}{2}AE^*(R^{\mathrm{H}})^{1/2}\alpha_{\mathrm{y}}^{1/2}. \tag{23}$$

So the general elastic plastic loading curve is

$$P = P_y + \frac{3}{2}AE^*(R^{\mathrm{H}})^{1/2}\alpha_{\mathrm{y}}^{1/2}(\alpha - \alpha_{\mathrm{y}})$$

elastic−plastic loading curve. (24)

Finally the elastic plastic unloading curve can be written as

$$P = AE^*\left(R_{\mathrm{p}}^{\mathrm{H}}\right)^{1/2}(\alpha - \alpha_{\mathrm{p}})^{3/2} \quad \text{unloading curve.} \tag{25}$$

Using again the Thornton assumption 2 (i.e. area equality when the maximum normal force is acting) for the equivalent elastic behaviour, one can find again the relation (14) between the elastic and elastic–plastic radii in the general contact case.

Again the intersection point between the loading and unloading curves (P^*, α^*) and the EHSL (P_{e}^* in terms of force) can be found in a recursive way with the equation system (24) and (25), when a plastic deformation limit is imposed.

Finally the wanted EHSL can simply be obtained when one knows the contact geometry, the materials and the admissible plastic deformation for the screw balls return system.

A meaningful test of the general theory is given by the recovering of the EHSL for a steel commercial bearing whose material and contact geometry is included into standard [1]. The EHSL given in this standard for the roller bearing, whose characteristics are collected into Table 1, is $p_{\max} = 4200\,\mathrm{N}$.

Table 1
Properties for a commercial bearing included into ISO 76

Property	Sphere	Internal raceway
Signed curvature radii (mm)	3.175, 3.175	3.302, −20
Yield tension (N/mm^2)	1800	1800
Poisson ratio	0.33	0.33
Young module (N/mm^2)	2.05E5	2.05E5

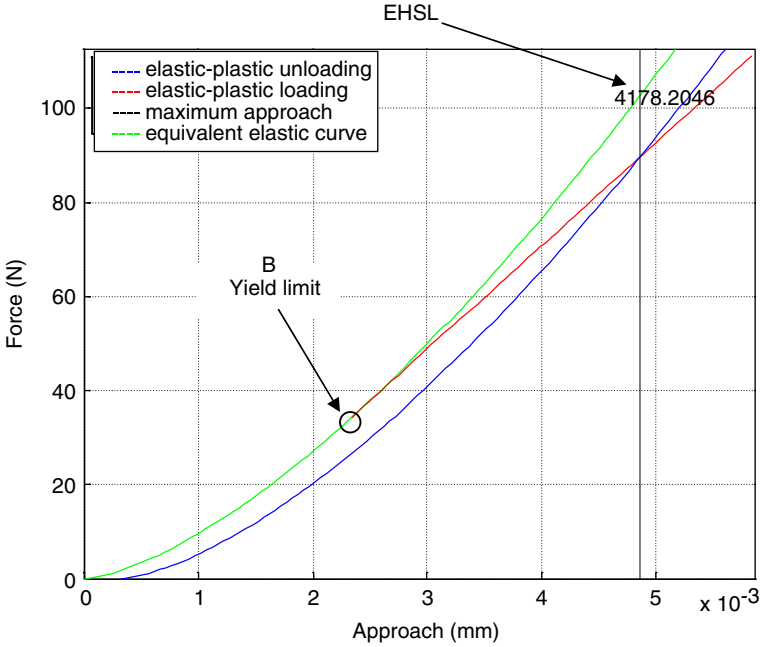

Fig. 5. EHL for a commercial bearing.

It is to note that the application of the general method to this bearing is presented in Fig. 5, if the steel deformation limit of ISO 76 standard, $\alpha_p = 0.0001 d_w$ is imposed, it is possible to find $p_{max} = 4178$ N that it is very close to the standard limit.

If the EHL is computed with the simplified theory of paragraph 2.1, the found limit for this geometry is 10% lower than the one that can be found with the whole theory presented in this paragraph.

The influence of the yielding stress on the EHSL is visible in the point B of Fig. 5 in terms of yield contact force.

3. Correlation between impact dynamic and contact force

As already demonstrated the presented theory is functional for the evaluation of the elastic–plastic stress limit through an EHSL valuable with simple-well know formulas. The found results are utilizable for a lot of different typologies of ball screw bearings and they have to be described through the typical kinematical parameters of a ball screw bearings, to be functional for the designer. So the already found limits have to be described in terms of an equivalent bearing with a *nominal contact angle between the sphere and the return system* (β) in degree, the *screw spinning velocity* in round per minute (n_A), *sphere distance from the screw centre* ($T/2$) see Fig. 6 on the right.

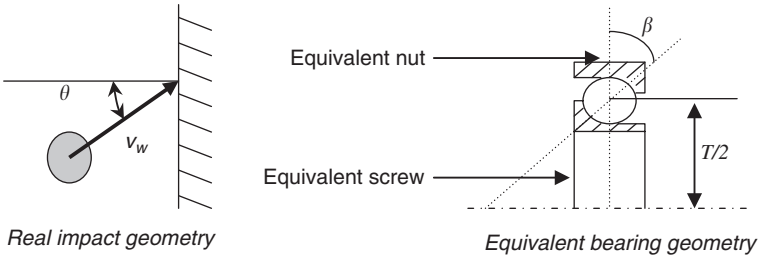

Fig. 6. Equivalent kinematical geometry for impact correlation.

Calling n_J the *nut spinning velocity* (usually equal to 0), the nominal impact velocity between the sphere and the return system is easy to obtain with the typical formula of the bearings kinematics [6]:

$$v_w = \frac{\pi \times d_w}{60 \times 1000}\left(\frac{T}{d_w} - \frac{\cos\beta}{T/d_w}\right)\frac{n_A - n_J}{2}\ (\mathrm{m/s}). \tag{26}$$

If an oblique impact has to be taken into account, one has only to compute the v_w component perpendicular to the return system (usually the nominal trajectory of the sphere is near to the one tangent to the return system), using the θ *impact angle* defined in Fig. 6 on the left:

$$v = v_w \cos\theta. \tag{27}$$

The impact between the two bodies can be considered as a centred impact (whose impact time is so much longer than if we consider the fundamental vibration period of the bodies) so that the impact elastic wave passes from the sphere to the return system and back to the sphere during the impact [13].

The impact law of motion, when the return system mass (m_{re}) is many times bigger than the sphere mass (m_{sp}), can be written as

$$\ddot{\alpha} = -P\frac{m_{\mathrm{re}} + m_{\mathrm{sp}}}{m_{\mathrm{re}} m_{\mathrm{sp}}} = -\frac{P}{m_{\mathrm{sp}}} = -\left(\frac{AE^*\left(R^{\mathrm{H}}\right)^{1/2}}{m_{\mathrm{sp}}}\right)\alpha^{3/2}, \tag{28}$$

where $\ddot{\alpha}$ is the approach acceleration, and the last term of Eq. (28) is written using Eq. (21).

The integration of Eq. (28) gives

$$\frac{1}{2}\left(\dot{\alpha}^2 - v^2\right) = -\frac{2}{5}\frac{AE^*\left(R^{\mathrm{H}}\right)^{1/2}}{m_{\mathrm{sp}}} 1\alpha^{5/2}. \tag{29}$$

By Imposing $\dot{\alpha} = 0$, zero approaching velocity, one can obtain the equivalent elastic maximum approach as

$$\alpha_{\max} = \left(\frac{5}{4}\frac{m_{\mathrm{sp}} v^2}{AE^*\left(R^{\mathrm{H}}\right)^{1/2}}\right)^{2/5}. \tag{30}$$

It is clear that for every geometry and material of both the sphere and return systems if one knows the $\alpha_{\max}$ it is possible to find first the P_{el} through Eq. (21) and then the EHS in order to evaluate if the *EHSL* is reached or less.

A simple validation of the initial hypotheses, long impact time, is feasible by the integration of Eq. (29).

Using the above formulas the designer is able to obtain a set of meaningful graphics displaying the correlation between the EHS, the screw spinning and the nominal impact angle.

In Fig. 7 one of these graphs is displayed, the characteristics of the screw balls bearing used are shown in Table 2, the computed EHLS for this screw balls bearing is $p_{\max} = 3121\mathrm{N/mm}^2$.

The graphs like the one below is very important for two different reasons: if the EHSL is known it is possible to define a lot of different impact angle-screw spinning couples to design the new return system, if an unwanted failure is detected during the test phase very confident hypotheses on real contact geometry can be done (usually the EHSL and the screw spinning velocity are known so the real impact angle can be found).

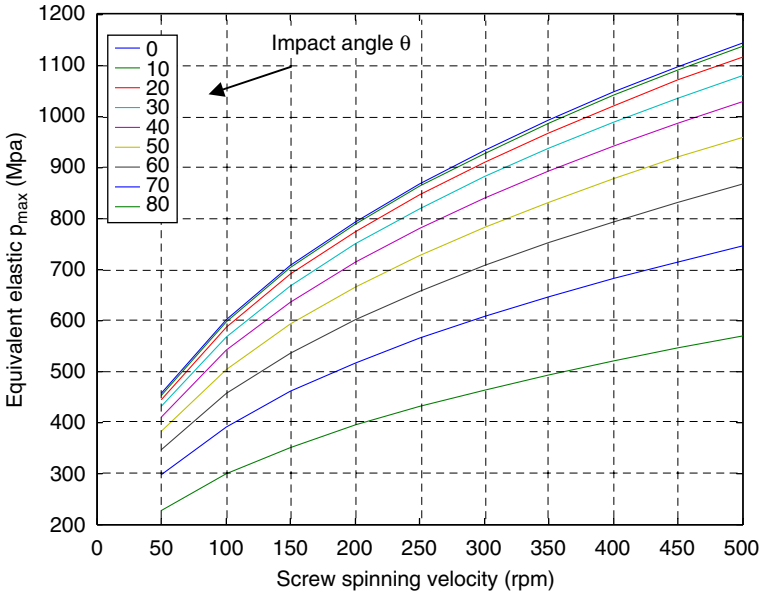

Fig. 7. EHS for a commercial screw balls bearing.

Table 2
Properties for the commercial screw balls bearing of Fig. 7

Property	Sphere	Return system
Signed curvature radii (mm)	2	−2.1 −17,4
Yield tension (N/mm^2)	1800	1138
Poisson ratio	0.33	0.33
Young module (N/mm^2)	2.05E5	2.05E5
Density (kg/m^3)	7850	7850
Nominal contact angle (deg.)		45°

In some industrial application where the nut stiffness is considerably reduced by the return system cut, one can find, using this latter graph, that the nominal contact angle for internal return systems (that is usually up to 75°), can reach the 0° value due to elastic deformation under external loads. So a resulting static failure is observed after a few hours of life.

It is important to note that, if an excessive plastic deformation is reached for a single load step during the testing phase, the impact geometry in the beginning of the return system is changed permanently and the contact cannot return in the "nominal state".

Another very important design graph is the one that can be built showing the maximum admissible spinning velocity in relation to the impact angle and the yield stress of the return system (see Fig. 8, for a commercial screw ball with the nominal geometry of Table 2).

4. Equivalent Hertzian stress limit of innovative materials

The already presented general theory is able to predict EHSL also for different materials, as ceramics and PEEK, if the plastic approach limit α_p is known.

Some meaningful considerations on screw maximum spinning velocity obtainable for a given geometry and different materials can be done using the so called *yielding velocity* (v_y), that is the velocity of the screw when the yield contact pressure is reached for the sphere-plane configuration, see Eq. (7) again.

If the screw spinning is under the v_y, the restitution factor for the impact is equal to one and it is possible to describe the correlation between the yield velocity and the return system materials and geometry. For an

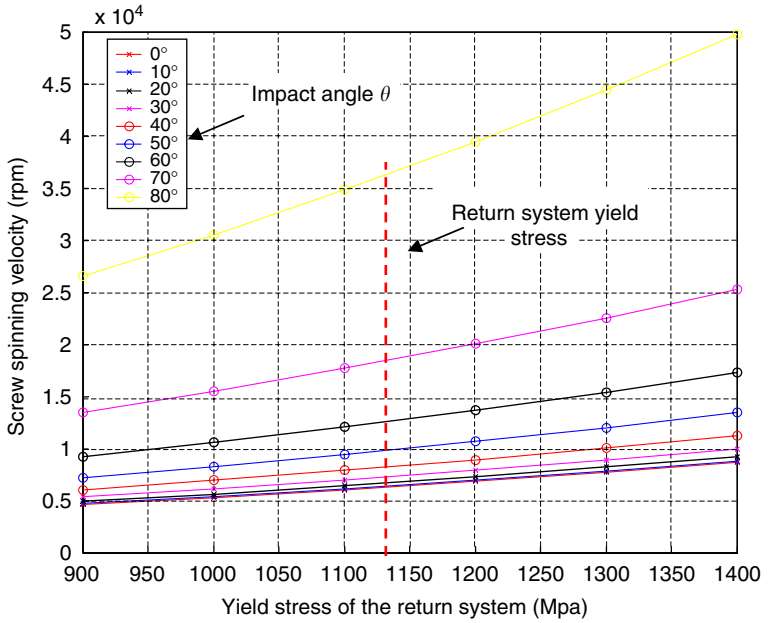

Fig. 8. Maximum screw spinning velocity for a commercial screw balls bearing.

impact angle equal to zero it is possible to find v_y like in [8,11], using the simple theory of paragraph 2.1:

$$v_{\mathrm{y}} = 3.194\left(\frac{(\sigma_{\mathrm{y}})_{\mathrm{th}}^{5}(R^{*})^{3}}{(E^{*})^{4}m_{\mathrm{sp}}}\right)^{1/2} \tag{31}$$

where the $(\sigma_{\mathrm{y}})_{\mathrm{th}}$ Thornton yield stress is the maximum pressure acting on contact surface when the yield stress is reached on the raceway skin. From the works by Thornton et al., see [14,15], we can find $2.4\,\sigma_{\mathrm{y}} < (\sigma_{\mathrm{y}})_{\mathrm{th}} < 2.4\,\sigma_{\mathrm{y}}$ and the flattening reaches the skin (see again Fig. 2) at the value $(\sigma_{\mathrm{y}})_{\mathrm{th}} = 2.4\,\sigma_{\mathrm{y}}$.

The yield stress velocity is very important for the estimation of the *impact elastic limit* (i.e. the strongest impact that produces no plastic deformation) and this simple relationship is also valid for curved geometry comparison using different materials if we want to identify the correlation between the v_{y} and all the other parameters.

From Eq. (31) it is possible to see that the yielding velocity, for a given geometry R^{*}, is proportional to the fifth power of the $(\sigma_{\mathrm{y}})_{\mathrm{th}}$ and inversely proportional to the fourth power of the Young modulus and to the sphere mass.

Looking at Eq. (31) it is possible to find similar value of yielding velocity for very different couple of materials, i.e. very different couple of materials for spheres and return system may have similar v_{y}.

Especially in aeronautical application it is possible to take into account a screw ball bearing with ceramic spheres and PEEK return system, the $(\sigma_{\mathrm{y}})_{\mathrm{th}}^{5}/(E^{*})^{4}$ ratio for PEEK is not so different from the steel one and the mass of the spheres is reduced a lot. Moreover if "plastic" materials for the return system are introduced a considerable advantage is reached during the production of the return system in respect to the steel return system that is very difficult and very expensive to produce.

In Fig. 9 it is possible to see the yield velocity for a steel return system—steel sphere screw ball bearing (steel–steel) drawn for different values of yield stress and Young modulus of the return system. The 3D graph is presented on the left while the same graph is presented with a 2D sliced representation of the previous one on the right.

In Figs. 10 and 11 the same graphs are presented for a peek return system—steel sphere (peek-steel) and for a peek return system—ceramic spheres (peek-ceramic).

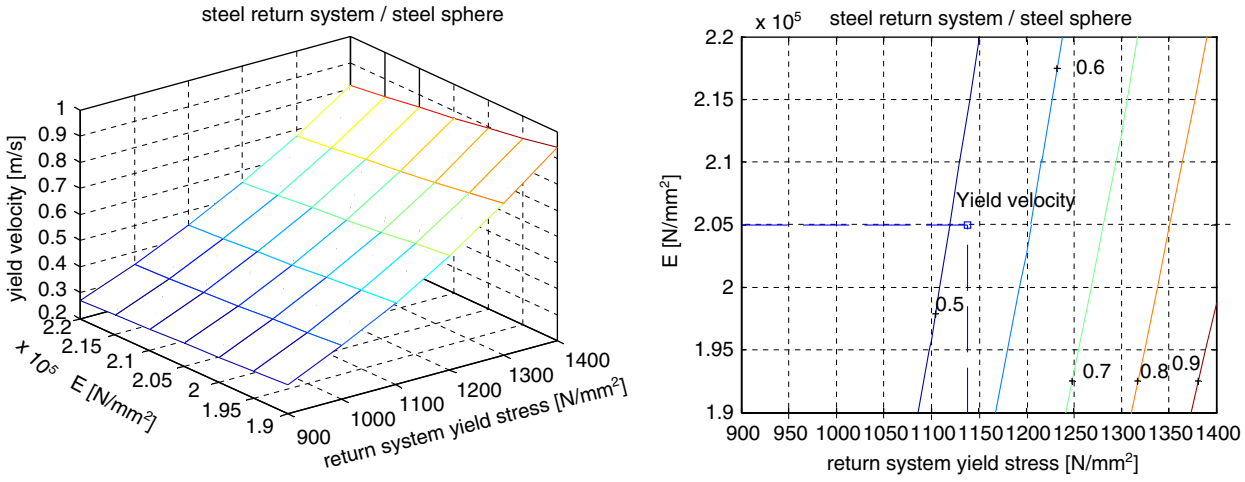

Fig. 9. Yield velocity for a steel return system—steel sphere screw ball bearing.

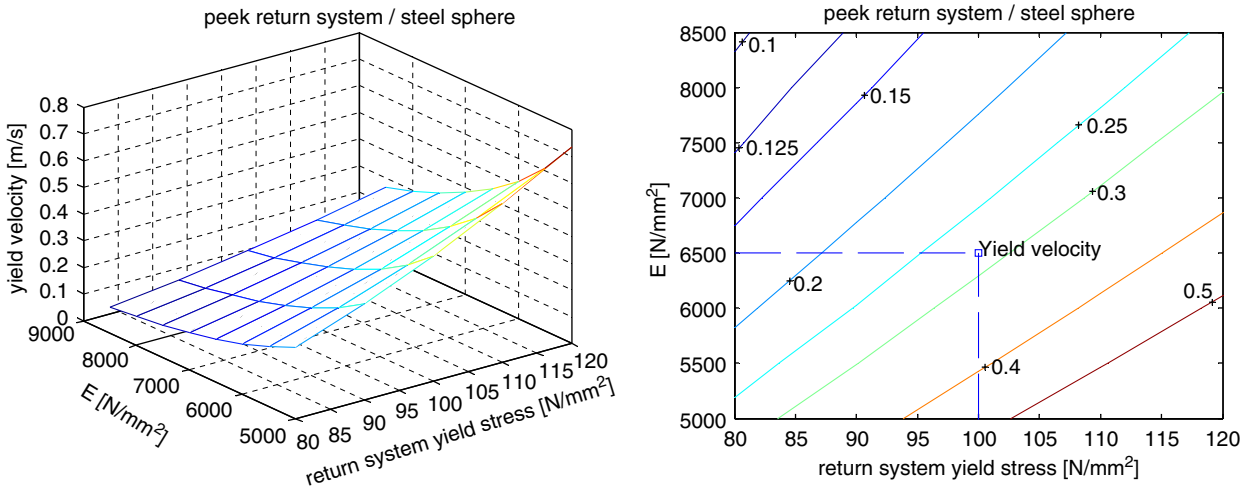

Fig. 10. Yield velocity for a peek return system—steel sphere, screw ball bearing.

Using the typical values for steel, ceramic and peek of Table 3 it is possible to make the following consideration: the yield velocity for a steel–steel system is 0.519 m/s, for the peek–steel system is 0.281 m/s and for peek–ceramic system is 0.484 m/s. So the yield velocity of the peek–steel system is the 54% of the steel–steel one, but if ceramic spheres are used the ratio increases to 93%, see again the mass contribute into Eq. (31). Looking at these values one can conclude that for a lot of commercial configuration the utilization of these new materials is possible because of the good yield velocity reacheable.

If the plastic admissible deformation α_p were known through experimental testing also for other materials (e.g. peek and bronze) a lot of different very powerful diagrams could be drown.

If the geometry of Table 2 is used with an impact angle of 76° and a screw spinning velocity of 2000 RPM, imposing, only for explanation purpose, an equal $\alpha_p = 0.0001\, d_w$ for all the three return system materials (steel, bronze and peek) it is possible to draw a graphic for all the suitable materials configuration for any given geometry.

In Fig. 12 the EHS for every couple of interesting return system—sphere material is reported in terms of stress, in the same figure also the EHSL for every couple and the EHS/EHSL ratio is shown.

Using this simple diagram one can note that also if the same α_p is used, the peek–steel ratio (0.48945) is not so different from the steel–steel one (0.35275).

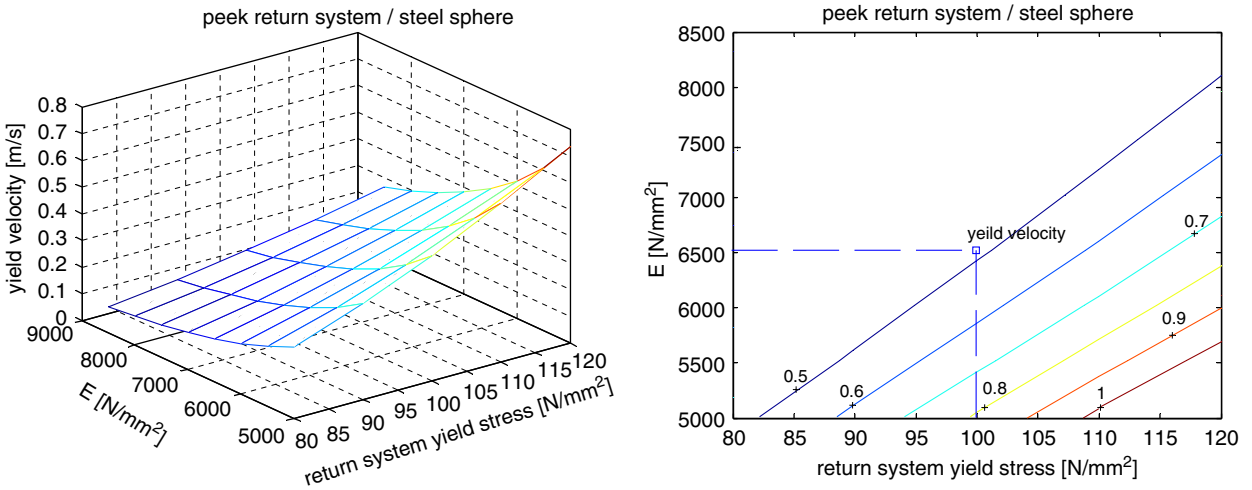

Fig. 11. Yield velocity for a peek return system—ceramic sphere, screw ball bearing.

Table 3
Properties for the screw ball bearing used in Figs. 9, 10 and 11

Property	Steel	Ceramic	PEEK	Bronze
Yield stress (N/mm^2)	1138	3000	100	565
Poisson ratio	0,33	0,26	0,3	0,312
Young modulus (N/mm^2)	2,05E5	3,0E5	6,5E3	1,1E5
Density (kg/m^3)	7850	3200	1400	7890
Sphere diameter	3.175	3.175	3.175	3.175

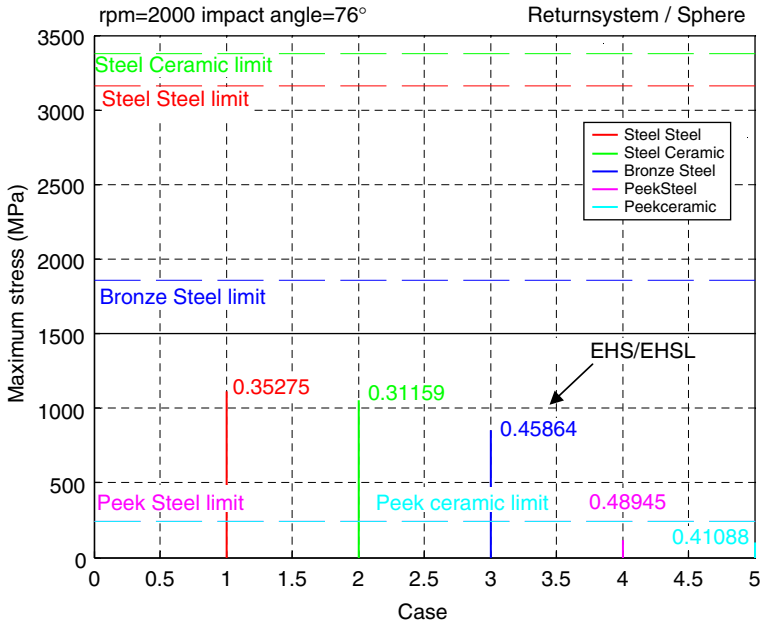

Fig. 12. EHS and EHSL for different couples of materials.

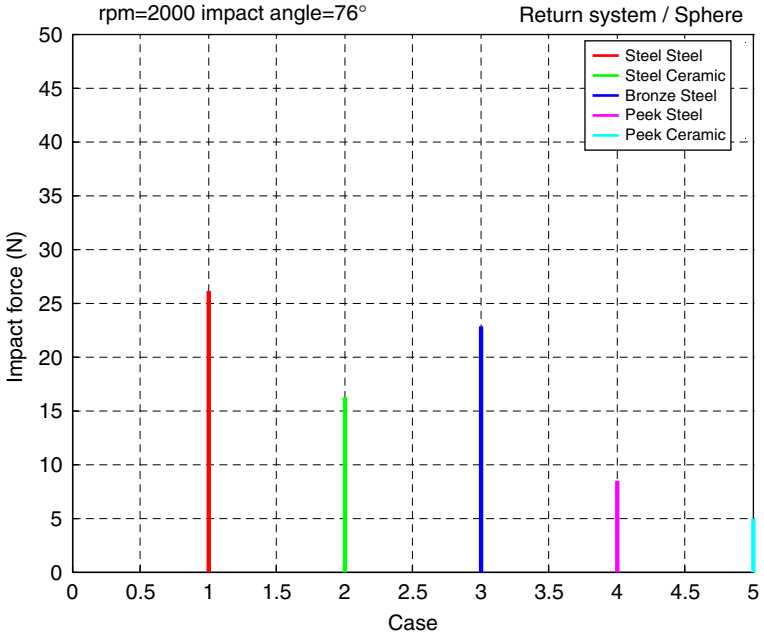

Fig. 13. Impact force for a given geometry with different materials.

In Fig. 13 the same results are presented in terms of impact force (N), that is another very meaningful design parameter.

Looking at these graphs it is possible to conclude once again that for a lot of different industrial components different sets of material couples are utilizable. It is to say that, for a confident comparison, the different "real" plastic deformation limits have to be computed through experimental tests.

5. Conclusions

In this paper, an elastic–plastic model for impact analysis on ball screws return system has been presented, to determine the elastic–plastic stress limit on the return system. The impact stress limit, often due to "fast" incremental plastic deformation on the beginning of the return system, is described through an Equivalent Hertzian Stress, based on the maximum tolerable plastic deformation. This tolerable deformation has to be established through experimental tests for a given return system material. Using this EHSL the design and validation of new return system configurations can be conducted using the well-known, simple Hertz elastic formulas.

Moreover some very meaningful graphics correlating the typical kinematical parameters of a ball screw bearings system and the already founded limits were presented. At least, a comparison between screw maximum spinning velocity obtainable for a given geometry and different materials, can be done using the so-called yielding velocity. Using the yielding velocity parameter comparison it is possible to assume the suitability of new "light" materials solutions for aeronautical components.

References

[1] ISO 76—Rolling bearing—Static Load Ratings.
[2] Hertz H. Uber die Beruhrung fester elastischer Korper (On the contact of elastic solids). J Reine Angewandte Math 1882;92:156–71.
[3] http://www.umbracus.com/umbra_spa/Download/TB_technical_Descripton.pdf.
[4] Draft standard DIN 69051-4, Publication date:1989-04—Machine tools; ball screws; computation of static and dynamic load ratings and life.

[5] Changsen W. *Analysis of rolling bearings*. London: Mechanical Engineering Publications Ltd; 1991.
[6] Viventi F. Valutazione dell'influenza del ricircolo nel moto delle viti a ricircolazione di sfere. Final dissertation facoltà di Ingegneria, Università di Perugia A.A. 2001/2002.
[7] Thornton C. Coefficient of restitution for collinear collisions of elastic perfectly plastic spheres. ASME J Appl Mech 1997;64:383–6.
[8] Thornton C, Ning Z. A theoretical model for the stick/bounce behaviour of adhesive, elastic–plastic spheres. Powder Technol 1998;99:154–62.
[9] Vu-Quoc L, Zhang X, Lesburg L. Contact force–displacement relations for spherical particles accounting for plastic deformation. Int J Solids Struct 2001;38(36–37):6455–90.
[10] Zhang X, Vu-Quoc L. Modeling the dependence of the coefficient of restitution on the impact velocity in elasto-plastic collisions. Int J Eng 2002;27:317–41.
[11] Hussainovaa I, Barseppa J, Shcheglovb I. Investigation of impact of solid particles against hard metal and cermettargets. Tribol Int 1999;32:337–44.
[12] Timoshenko S, Goodier JN. Theory of elasticity, 3rd ed. McGraw Hill; 1970.
[13] Hung JP, Wu JS, Chiu JY. Impact failure analysis of re-circulating mechanism in ball screw. Eng Failure Anal 2004;11:561–73.
[14] Wu C, Li L, Thornton C. Rebound behaviour of spheres for plastic impacts. Int J Impact Eng 2003;28:929–46.
[15] Mishra K, Thornton C. An improved contact model for ball mill simulation by the discrete element method. Adv Powder Technol 2002;13:25–41.